Cullin-5 mutants reveal collective sensing of the nucleocytoplasmic ratio in Drosophila embryogenesis

(Article begins on next page)

07 July 2024

Cullin-5 regulates nuclear positioning and reveals insights on the sensing of the nuclear-to-cytoplasmic ratio in *Drosophila* embryogenesis

Luke Hayden[1], Anna Chao[1], Victoria E. Deneke[1^], Alberto Puliafito[2,3], and Stefano Di Talia[1*]

[1]Department of Cell Biology, Duke University School of Medicine, Durham, NC 27710, USA

^ Present address: Research Institute of Molecular Pathology (IMP), Vienna BioCenter (VBC), Campus-Vienna-Biocenter 1, 1030 Vienna, Austria

[2]Candiolo Cancer Institute, FPO-IRCCS, Laboratory of Cell Migration, Candiolo, 10060, Italy

[3]Department of Oncology, Università di Torino, Candiolo, 10060, Italy

[*]Correspondence: stefano.ditalia@duke.edu

Summary

In most metazoans, early embryonic development is characterized by rapid division cycles which pause before gastrulation at the mid-blastula transition (MBT).[1] These early cleavage divisions are accompanied by cytoskeletal rearrangements which ensure proper nuclear positioning. Yet, the molecular mechanisms controlling nuclear positioning are not fully elucidated. In *Drosophila*, early embryogenesis unfolds in a multinucleated syncytium, and nuclei rapidly move across the anterior-posterior (AP) axis at cell cycles 4-6 in a process driven by actomyosin contractility and cytoplasmic flows.[2,3] Previously, *shackleton* (*shkl*) mutants were identified in which this axial spreading is impaired.[4] Here, we show that *shkl* mutants carry mutations in the *cullin-5* (*cul-5*) gene. Live imaging experiments show that Cul-5 is downstream of the cell cycle but required for cortical actomyosin contractility. The nuclear spreading phenotype of *cul-5* mutants can be rescued by reducing Src activity genetically, suggesting that a major target of Cul-5 is Src kinase. *cul-5* mutants display gradients of nuclear density across the AP axis at the MBT which we exploit to study cell cycle control as a function of the N/C ratio. We found that the N/C ratio is sensed collectively in neighborhoods of about 100μm and such collective sensing is required for a precise MBT in which all the nuclei in the embryo pause their division cycle. Moreover, we found that the response to the N/C ratio is slightly graded along the AP axis. These two features can be linked to the spatiotemporal regulation of Cdk1 activity. Collectively, our results reveal a new pathway controlling nuclear spreading and provide a quantitative dissection of how nuclear cycles respond to the N/C ratio.

Keywords

Nuclear positioning, actomyosin contractility, Mid-blastula transition, nuclear-to-cytoplasmic ratio, Cullin-5, Src

Results

shkl encodes the ubiquitin ligase cullin-5

shkl mutants are among the few genetic perturbations which have been shown to directly impinge on the spreading of nuclei in early *Drosophila* embryogenesis.[4,5] Moreover, shkl embryos display gradients in nuclear density, which have been linked to a significant decrease in the synchrony of the last cell cycle preceding the MBT.[3] To elucidate how shkl regulates nuclear positioning and how such regulation impacts cell cycle lengthening at the MBT, we first obtained two shkl alleles identified in the original mutagenesis screen (shkl^GM130 and shkl^GM163) and imaged embryos laid by transheterozygous mothers (hereinafter shkl embryos). We confirmed that in shkl embryos the nuclear cloud failed to reach the posterior pole of the embryo at the correct time and nuclei were not positioned uniformly, as seen previously (Fig. 1A-B).[4] Moreover, we found that the lower density of nuclei in the posterior of the embryo was frequently accompanied by an extra round of nuclear divisions (Supplementary Movie 1). Thus, failures in nuclear positioning can have significant impact on the collective and synchronous decision of all nuclei to remodel the cell cycle at the MBT.

To identify the shkl gene, we used a DNA sequencing approach, centered on the fact that the original screen was performed in a strain carrying an isogenic third chromosome and that two alleles of the shkl gene were available.[4] We reasoned that the third chromosomes of these two

alleles had little time (~20 years) to accumulate mutations with respect to each other. Thus, we predicted that genomic sequencing of *shkl* flies (*shkl*[GM130]/*shkl*[GM163]) would show a much lower number of heterozygous single nucleotide polymorphisms (SNPs) than homozygous ones relative to the reference genome on the third chromosome, a prediction which we could readily confirm (Fig. 1C). Taking advantage of the low number of heterozygous SNPs and the previous mapping[4] of *shkl* between two markers (*ebony* and *claret*) on the right arm of chromosome 3, we looked for genes that carried two heterozygous missense SNPs with the idea that this would narrow our search to only a handful of genes (Fig. 1D). Bioinformatics analysis confirmed the validity of this argument, and we identified *cullin-5* (Cul-5) as the best candidate as allele *shkl*[GM163] carried a premature stop codon at amino acid 51 and *shkl*[GM130], a missense mutation (E to K) in the very conserved neddylation domain, a domain required for ubiquitin ligase activity and which is well-conserved across evolution (Fig. 1E).[6] To perform complementation and rescue experiments, we fixed and stained embryos with DAPI to estimate the extent of nuclear spreading by measuring the shape of the nuclear cloud in cell cycle (cc) 6. We found that *shkl* alleles failed to complement an available *cullin-5* mutant (Fig. 1F). In addition, maternal expression of *cullin-5* from the *twine* promoter (which drives expression specifically in the germline[7]) was able to significantly rescue the nuclear spreading defects (Fig. 1F). Collectively, these results identify *shkl* mutants as alleles of the *cullin-5* genes and demonstrate that maternal expression of *cullin-5* is important for nuclear positioning in *Drosophila* embryos.
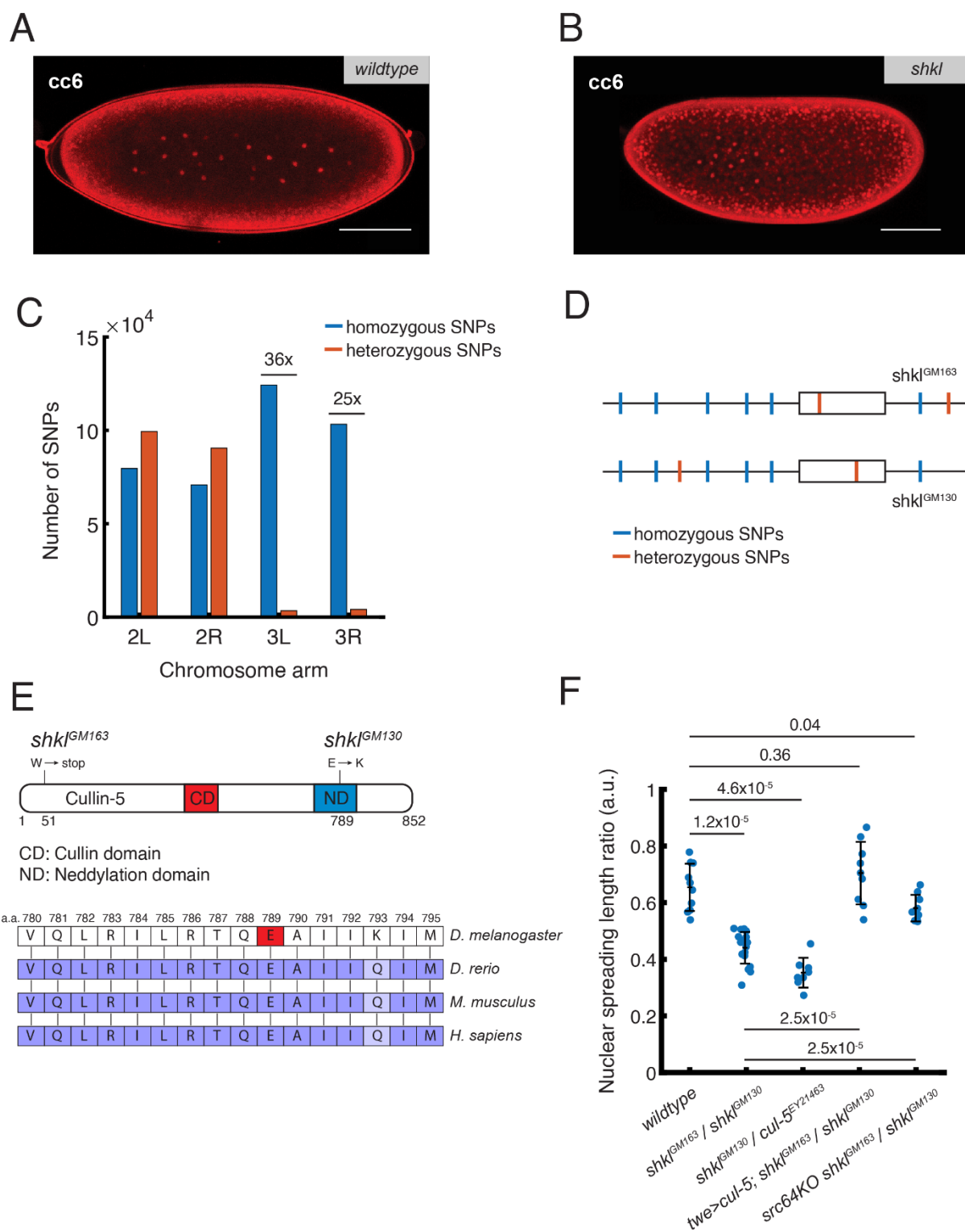
Fig. 1. Genetic identification of *shkl* mutants. (A, B) Nuclear positioning in interphase of cc 6 in wildtype (A) and *shkl* (B) embryos, visualized with PCNA-TagRFP. (C) Number of

homozygous and heterozygous SNPs (relative to the reference genome) in *shkl* embryos in each arm of chromosome two and three. The mutant screen[4] was performed on an isogenic third chromosome and thus only the third chromosome has reduced heterozygous SNPs. (D) A theoretical example gene with heterozygous SNPs between the two *shkl* alleles. (E) Top: Schematic for the Cul-5 protein with domains and *shkl* mutations shown. The *GM130* allele of *shkl* contains a point mutation in the neddylation domain where it is evolutionarily conserved. The *GM163* allele contains a point mutation leading to an early stop codon. Bottom: Part of the neddylation domain of the Cul-5 protein in different model organisms. Highlighted residue indicates *GM130* mutation site. (F) Genetic complementation and rescue tests. Fixed embryos were stained with DAPI to show nuclear positioning at cc 6. The ratio between the length of the nuclear cloud and the length of the embryo was measured. Data are represented as mean ± SEM. P-values (Kolmogorov–Smirnov test) are shown. Each dot represents one embryo. *cul-5*^{EY21463} is a hypomorphic mutant allele. twe>cul-5 is a transgenic line carrying a plasmid with cul-5 cDNA under the regulation of the twine promotor. Scale bar: 100µm.

shkl is downstream of the cell cycle and regulates cortical contractility

1   In our previous work, we showed that nuclear spreading is driven by cytoplasmic flows generated

2   by cortical actomyosin contractility, which is in turn controlled spatiotemporally by the cell cycle

3   oscillator (Fig. 2A).[3] To quantify the degree to which cytoplasmic flows are disrupted in *shkl*

4   embryos, we used yolk autofluorescence images to perform particle image velocimetry (PIV) in

5   live embryos also expressing PCNA-TagRFP (which allows visualization of nuclei deep in the

6   embryo) and measured the velocity of the cytosol and nuclei during the early cell cycles when

7   axial expansion occurs. As previously shown, the wildtype embryos showed strong cytoplasmic

6

8   flows coupled with nuclear movement which spread the nuclei across the anterior-posterior (AP)

9   axis by the end of cell cycle 6 (Fig. 2B, D, S1).[3] In contrast, cytoplasmic flows and nuclear

10   movement in *shkl* embryos were sharply reduced (Fig. 2C, E, S1). Since cytoplasmic flows are

11   generated by recruitment of active Myosin II to the cortex by active Rho,[3,8] we sought to determine

12   if the activities of these regulators are perturbed in *shkl* embryos. To that end, we measured the

13   dynamics of a Rho biosensor[9] and myosin II recruitment to the embryo cortex. Both Rho activity

14   (Fig. 2F, S1) and myosin II recruitment (Fig. 2G) were reduced in *shkl* embryos as compared to

15   wildtype. Next, we analyzed whether Cul-5 might impact actomyosin contractility by regulating

16   the cell cycle. To this end, we looked at the master regulator Cdk1 by measuring the Cdk1-to-PP1

17   activity ratio using a FRET-based biosensor in both wildtype and *shkl* embryos.[10,11] The

18   oscillations in the activity ratio were similar in wildtype and *shkl* embryos. Moreover, the duration

19   of the cell cycle near the middle of the embryo was also essentially unaltered (Fig. 2H, S2).

20   Therefore, we argue that Cul-5 does not regulate the cell cycle oscillator. Taken together, our

21   results indicate that Cul-5 is necessary for the proper activity of Rho and recruitment of myosin II

22   which in turn regulate cortical contractility and nuclear positioning.
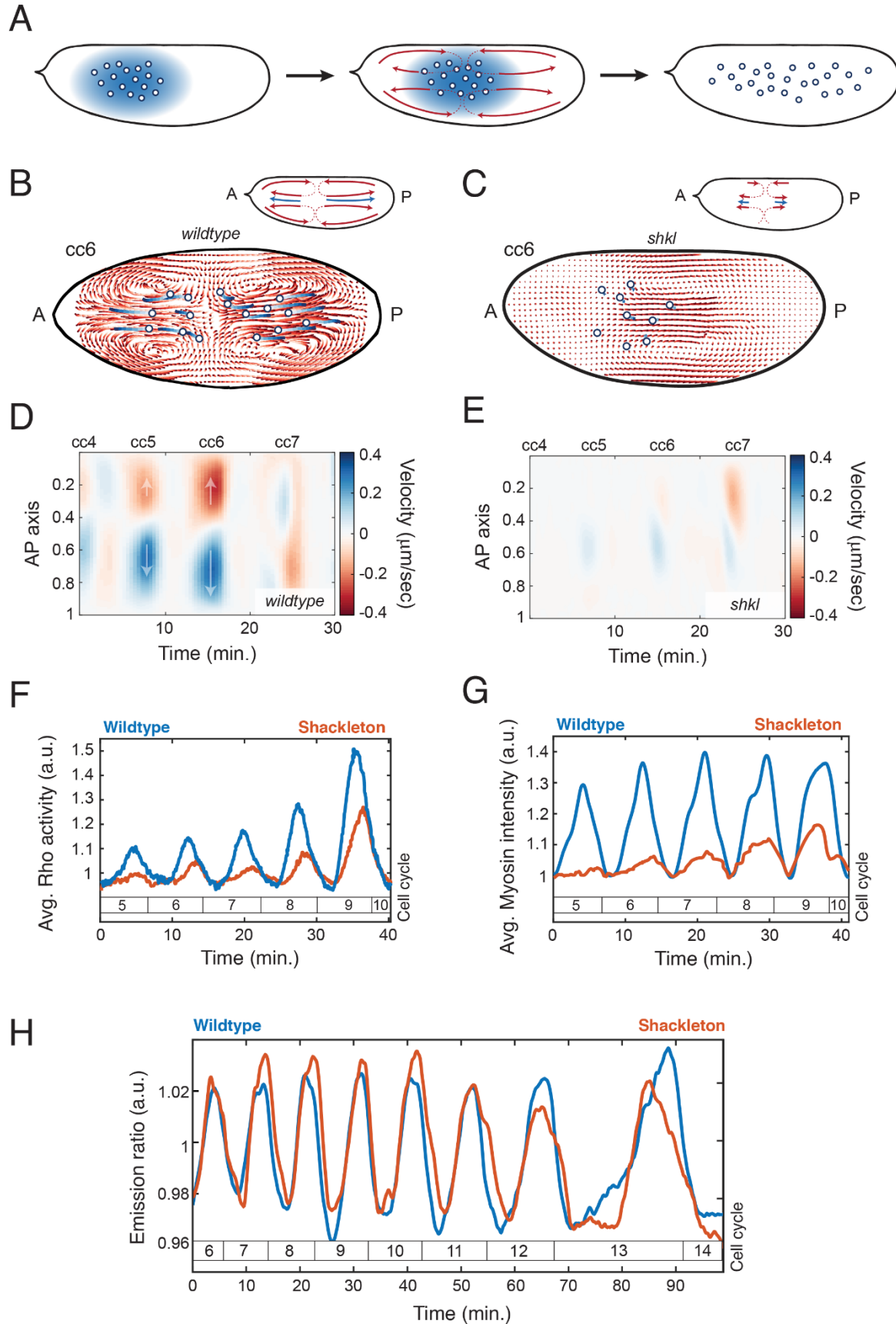
24 **Fig. 2. Characterization of the Cul-5 pathway.** (A) Pathway for self-organized nuclear

25 positioning in wildtype embryos; PP1 activity spreads from nuclei to the embryo cortex where it

26 leads to gradients of myosin accumulation, thus generating cytoplasmic flows. These flows

27 position nuclei uniformly across the AP axis. (B, C) PIV in wildtype (B) and *shkl* (C) embryos

28 showing reduced cytoplasmic flows and nuclear movement in *shkl* embryos. Top insets depict

29 magnitude and directionality of flows. (D, E) Heatmap quantification of the cytoplasmic flows in

30 wildtype (D) and *shkl* (E) embryos. Arrows depict directionality of flows. (F, G) Both cortical Rho

31 activity (F) and cortical myosin accumulation (G) are reduced in *shkl* embryos. (H) Cortical

32 oscillations of the Cdk1/PP1 ratio from the FRET biosensor are similar in wildtype and *shkl*

33 embryos.

34

Cul-5 regulates cortical contractility through restricting the activity of Src.

36 Cul-5 is a ubiquitin ligase which works in conjunction with other factors to regulate protein

37 stability.[12] A major target of Cul-5 is Src kinase[13-15], whose activity is restricted by several

38 ubiquitin ligases.[16-18] Src is known to regulate the cytoskeleton[19,20], including actomyosin

39 contractility.[21] These observations suggest that Cul-5 could (at least partly) regulate the axial

40 expansion process by restricting Src activity. To test this hypothesis, we performed experiments

41 using the Gal4/UAS system to overexpress constitutively active forms of the two Src homologs in

42 *Drosophila*, Src42A or Src64B.[22] We saw that overexpression of either homolog is sufficient to

43 recapitulate the *shkl* phenotype with sharply reduced cytoplasmic flows and nuclear spreading (Fig

44 S1). Similarly, if *shkl* embryos have reduced cortical contractions due to excessive Src activity,

45 then genetically decreasing Src activity should rescue the *shkl* phenotype. We examined *shkl*

46 mutants which also had only one copy of Src64B (heterozygous for *Src64B*^{KO}, described

47   previously[20]) and quantified cytoplasmic flows and nuclear positioning. We saw that reducing Src

48   activity in *shkl* embryos significantly reduced the defects in axial expansion (Fig. 1F). Collectively,

49   these results implicate the Cul-5/Src cascade in the regulation of nuclear positioning in *Drosophila*
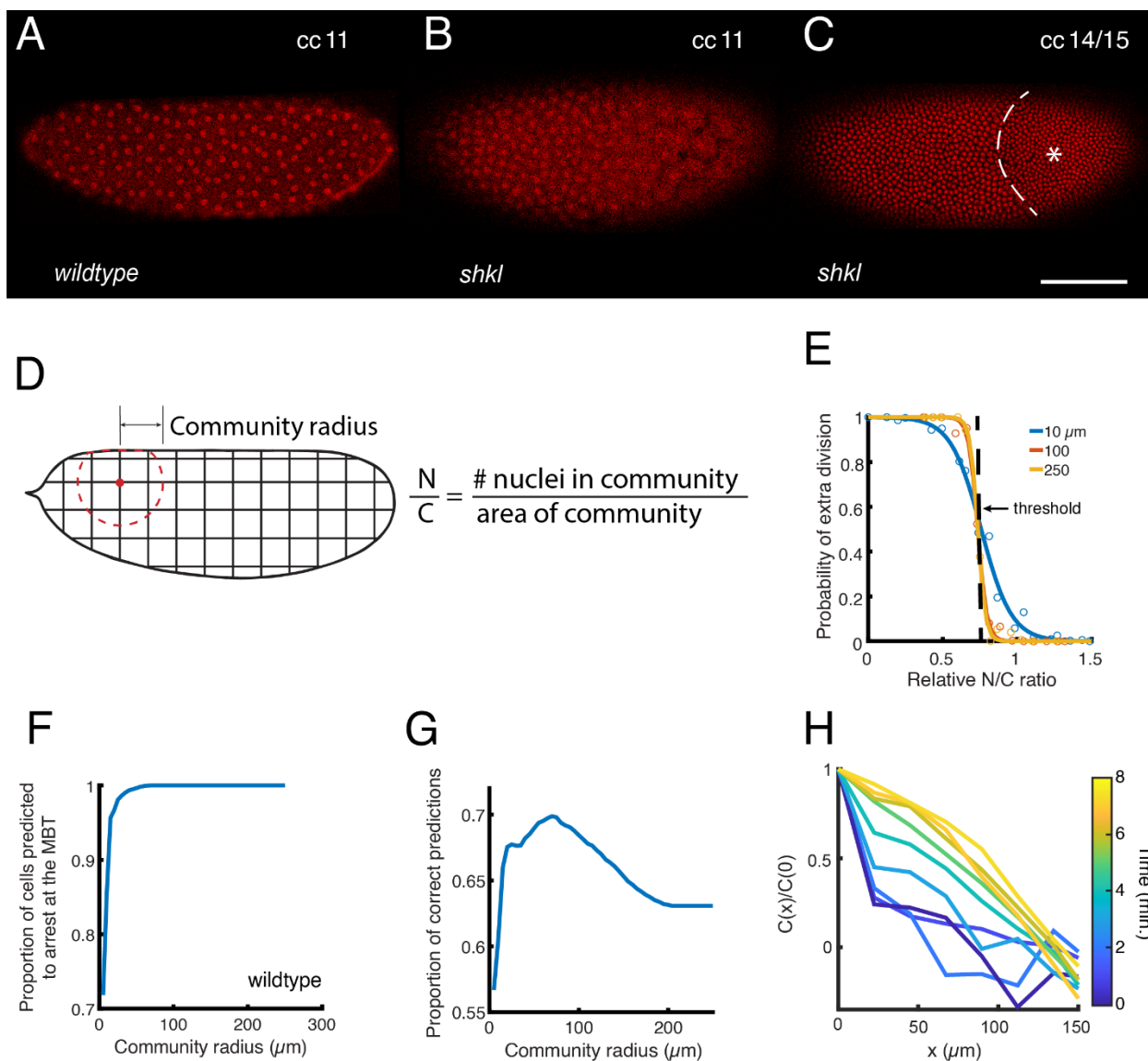
50   embryos.

51

52   **Nuclei sense the local nuclear density in large groups to determine whether to divide**

53   In wildtype embryos, the morphogenetic processes driving nuclear positioning ensure that nuclear

54   density is rather uniform across the embryo.[3] Since nuclear divisions are synchronized within

55   minutes[10,23] by Cdk1 waves,[10,24] nuclear density increases in 2-fold increments, which likely

56   facilitates the consistent cell cycle lengthening observed in all nuclei at the MBT. To gain insights

57   on how the embryo can achieve a robust response to changes in the N/C ratio, we observed that

58   the nuclear spreading defects in *shkl* embryos cause a nuclear density gradient across the AP axis

59   with lower density at the posterior (Fig. 3A-B, Fig. 4A). Therefore, we exploited this gradient to

60   probe the response to gradual changes in nuclear density. We observed that the lower density of

61   nuclei in the posterior of the embryo is frequently accompanied by an extra round of nuclear

62   division (Fig. 3C). Interestingly, the size of the region which does an extra division varies across

63   embryos and is frequently less than half the size of the embryo. Moreover, a salt-and-pepper

64   phenotype with many regions of extra divisions next to regions of normal divisions is never

65   observed.[25,26] These two observations suggest that the nuclei do not sense the N/C ratio globally

66   or in an autonomous manner, but rather they do so in a collective manner over some distance, here

67   called the community radius. To infer this radius, we divided embryos into grids, measured the

68   nuclear density within circles of different radii, and scored whether each grid point was within a

69   region of either normal or extra division (Fig. 3D). We then fit these curves to logistic equations

10

70   and used the N/C ratio at which the curves crossed 50% probability as the best N/C ratio threshold

71   predictor, above which we predict embryos do not divide (Fig. 3E). As previously reported, these

72   thresholds were around 70% of the wildtype cell cycle 14 nuclear densities.[25] This value is half-

73   way between the nuclear density at cell cycle 13 and 14, which likely contributes to the decision

74   of all nuclei to divide rapidly at cell cycle 13 and lengthen their cycle 14. Next, we asked what is

75   the fraction of nuclei that would fail to lengthen their cell cycle at the MBT as a function of the

76   community radius. We found that to ensure that all nuclei (>99%) undergo a collective pause at

77   the MBT, the response to the N/C ratio must be averaged over a community radius of at least 35μm

78   (Fig. 3F). Such a community would contain about one hundred nuclei, thus implying that a robust

79   cell cycle decision at the MBT requires a collective nuclear response.

80   Next, we tried to infer the optimal radius and a possible molecular mechanism for the

81   collective nature of the cell cycle decision. Using the estimated thresholds, we measured the

82   proportion of correct predictions made in a test data set of *shkl* embryos with regions of extra

83   division and saw a peak in correct predictions at a community radius of 70μm (Fig. 3G). Next, we

84   used the Cdk1/PP1 FRET biosensor to measure the correlation length of the Cdk1/PP1 activity

85   field from the two-point correlation function. We found that this length (about 100 μm) is similar

86   to the optimal community radius, thus suggesting that the collective decision of nuclei to undergo

87   an extra division or not might reflect the fact that Cdk1/PP1 activity in neighboring nuclei

88   influences each other (Fig. 3H). We have previously shown that spatial correlations in Cdk1/PP1

89   activity arises from the reaction-diffusion dynamics that drive the cell cycle during interphase.[24]

90   Thus, we conclude that the syncytial nature of the nuclear cycles coupled to the reaction-diffusion

91   properties of the cell cycle oscillator ensure that nuclei act as large collectives and that such

92   collective increase the robustness of the MBT.

93

Fig. 3. Sensing of the N/C ratio in *shkl* embryos. (A, B) Positioning of nuclei at cc 11 in wildtype

(A) and *shkl* (B) embryos, visualized with His-RFP. (C) A *shkl* embryo at the MBT. The gradient

of N/C ratio in *shkl* embryos frequently leads to the posterior undergoing an extra division. Dashed

line: boundary between the normal and extra division regions. Asterisk: The region of the embryo

which underwent an additional division. (D) Schematic of experimental design. Each embryo was

discretized in a grid and a region with a certain community radius was specified. The N/C ratio

was calculated as the number of nuclei in the community divided by the area. (E) The probability

101   of a region dividing as a function of the local N/C ratio, relative to the average N/C ratio in wildtype

102   embryos at cc 14. Curves for local neighborhoods of 10, 100, and 250µm are shown. A simple

103   predictive model is a constant N/C ratio threshold, shown as a dashed line. (F) The proportion of

104   nuclei in wildtype embryos which should arrest at the MBT as a function of the community radius.

105   (G) Proportion of correct predictions in a test data set of *shkl* embryos using a simple threshold

106   model as a function of community radius. (H) Two-point correlation function of the Cdk1/PP1

107   field as a function of distance for embryos in interphase of cell cycle 13. The correlation length

108   was estimated as the point at which the correlation reaches 0.5 at the last time point and occurs at

109   ~100µm. Scale bar: 100µm.

110

111   **A gradient in sensing of the N/C ratio improves the ability to predict nuclear behaviors**

112   While our previous results revealed the importance of collective N/C ratio sensing, we observed

113   that the frequency of correct predictions from the model was limited to ~70% (Fig. 3G), suggesting

114   that we might be missing some additional regulation of the MBT or some additional aspects of the

115   response to the N/C ratio. Thus, we sought to determine whether a more complex model, still

116   centered on the N/C ratio, would account for the incorrect predictions (see Supplementary Figure

117   3). Notably, we found that the errors in prediction were distributed in a gradient across the AP axis

118   (Fig. 4A), suggesting that nuclei might sense the N/C ratio differently depending on their location.

119   We therefore hypothesized that a slight gradient in the N/C ratio threshold (with some small

120   variance between embryos) would be a better predictor (Fig. 4B). With this model, we were able

121   to correctly predict ~90% of nuclear divisions with the best community radius of ~100µm (Fig.

122   4C). Moreover, most of the errors in this model accumulated very close to the border of the normal

13

123   and extra division regions (Fig. 4D), where we would expect that the ability of Cdk1 to propagate

124   spatially might influence the decision.[10,27,28]

125   To further test the idea that the posterior of the embryo has a slightly higher N/C ratio

126   threshold than the anterior, we compared the probability of nuclei dividing as a function of N/C

127   ratio in the anterior and posterior. As predicted, the posterior third of the embryo showed a higher

128   N/C ratio threshold than the anterior third (~8% higher, Fig. 4E) which was independent of the

129   community radius used (Fig. 4F). To control that the apparent gradient in N/C ratio response is not

130   due to cytoskeletal and/or other effects of reduced Cul-5 activity, we investigated the decision of

131   nuclei to arrest at the MBT when the N/C ratio in embryos (with uniform nuclear positioning) is

132   brought closer to the threshold by genetic manipulations. We reasoned that in these embryos the

133   proximity of the nuclear density to the threshold will result in a significant fraction of embryos

134   having an extra division. To this end, we imaged embryos generated by crossing wild type females

135   to males carrying compound chromosomes[25]. As a consequence, these embryos contained either

136   one extra or one fewer copy of either chromosome 2 or 3. The embryos with one fewer copy of

137   chromosome 2 or 3 have a DNA content (83% and 80% respectively) close to the 70% threshold

138   seen in wildtype and also frequently had regions of an extra nuclear division.[25] As in *shkl* embryos,

139   the posterior of the embryos featured a slightly higher threshold than the anterior (~2% increase

140   for chromosome 2 and ~8% increase for chromosome 3; Fig. 4G). In accordance, 100% (n=33) of

141   extra divisions began in the posterior. Since the community radius and the correlation length of

142   the Cdk1/PP1 field are both ~100μm, we expect there to be a correlation between the Cdk1

143   activation rate measured during S phase (Fig. 4H) and nuclear density in the compound

144   chromosome embryos. Indeed, we saw there was a correlation between the two, and the regions of

145   the embryo which underwent an extra division were clustered at a low DNA content and higher

146   Cdk1 activation rate (Fig. 4I).

147   To gain further insight on the slight gradient in the N/C ratio threshold across the AP axis,

148   we divided wildtype embryos into grids and measured the Cdk1 activation rate in neighborhoods

149   of each grid point at cc 13. We saw a slight but significant increase in the Cdk1 activation rate

150   across the AP axis (Fig. 4J) which was not due to differences in the N/C ratio (Fig. S4). Since the

151   increased duration of S phase at cc 13 is primarily due to the Cdk1 inhibition by Chk1[29-31], we

152   measured the Cdk1 activation rate in *chk1 chk2* mutants and saw that the gradient across the AP

153   axis was ablated (Fig. 4K, S4). Thus, our results argue that the response of the cell cycle to nuclear

154   density is not uniform across the embryo and that this difference might be dependent on the DNA

155   replication checkpoint.
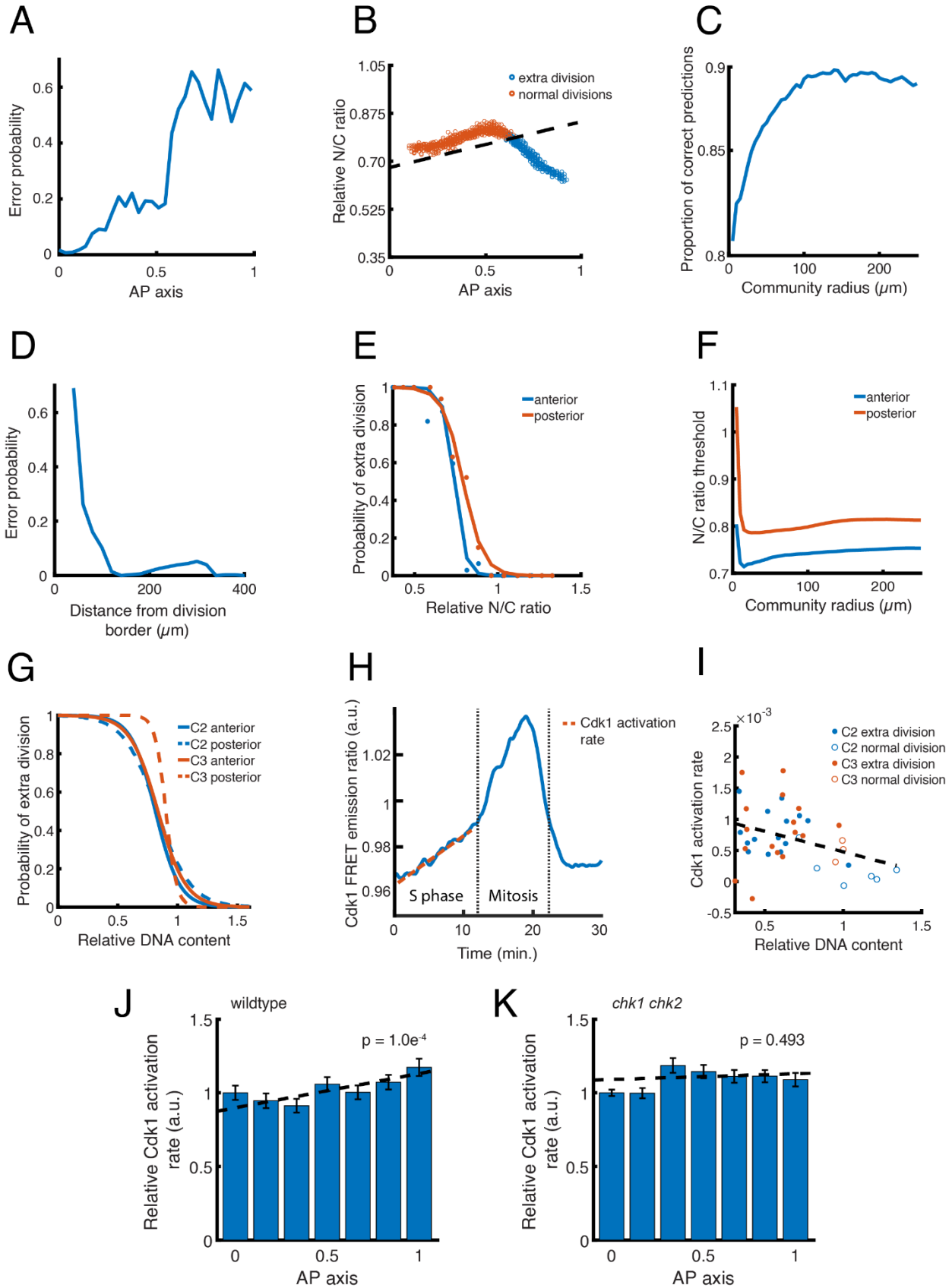
157 **Fig. 4. A gradient in N/C ratio sensing across the AP axis.** (A) Errors made by the simple

158 threshold model as a function of position across the AP axis. (B) The N/C ratio in local

159 neighborhoods of 70μm (the maximum of the correct predictions of the simple threshold model)

160 across the AP axis during cc 14. Dashed line shows that an N/C ratio threshold with a slight

161 gradient across the AP axis does a much better job at dividing the normal and extra division

162 regions. (C) This gradient threshold model predicts the division behavior correctly upwards of

163 90% of the time at a community radius of ~100μm. (D) Errors in prediction from the gradient

164 threshold model are largely near the border between normal and extra division regions. (E)

165 Probability of a region undergoing an extra division as a function of N/C ratio in the anterior third

166 versus posterior third of the embryo at a community radius of 100μm. The posterior curve is shifted

167 towards a higher N/C ratio. (F) The N/C ratio threshold in the anterior and posterior of the embryo

168 at different community radii. (G) Probability of a region undergoing an extra division as a function

169 of N/C ratio at a community radius of 100μm, performed in embryos with either one additional or

170 one fewer copy of either chromosome two or three. These embryos have altered DNA content but

171 normal nuclear spreading. (H) Diagram showing an oscillation of Cdk1/PP1 FRET ratio during cc

172 13. The dashed red line indicates a linear fit of the slope of the ratio during S phase which we use

173 as the Cdk1 activation rate. (I) Correlation between Cdk1 activation rate and division behavior in

174 normal and extra division regions in compound chromosome embryos. At low DNA content and

175 high Cdk1 activation rate, nuclei tend to divide. Dashed line: linear fit. (J, K) Cdk1 activation rate

176 across the AP axis (relative to the anterior of the embryo) in wildtype (J) and *chk1 chk2* (K)

177 mutants. Dashed lines indicate linear fit and p values (F-test) for the significance of the slope are

178 shown. Data are represented as mean ± SEM.

179

Discussion

The tight control of the cell cycle and nuclear (cell) positioning and number is a ubiquitous feature of metazoan development and is crucial to the proper development of early embryos. A self-organized mechanism ensures uniform nuclear positioning across the AP axis in *Drosophila* embryos and thereby a synchronous halt at the MBT prior to gastrulation.[3] In this work we have taken advantage of *shkl* mutants which have defects in nuclear spreading to identify a novel pathway involved in the control of cortical contractility and gain insights into how nuclei respond to changes in the N/C ratio.

Through DNA sequencing and complementation tests, we have identified *shkl* mutants as mutations of the ubiquitin ligase Cul-5. In the early embryo, Cul-5 does not regulate the cell cycle oscillator but is required for Rho and myosin activity. In many systems Cul-5 restricts the levels of active Src kinase[13-15], which is a known regulator of the actomyosin cytoskeleton. Indeed, we found that the *cullin-5* phenotype could be largely rescued through a genetic reduction in Src activity and recapitulated through Src overexpression, indicating that a main function of Cul-5 is to downregulate Src activity. These results implicate the Cul-5/Src axis as a crucial pathway involved in the control of cortical contractility in early *Drosophila* embryos.

In the early embryo, nuclei regulate their own positioning through PP1 activity which spreads from the nuclei to the cortex.[3] This localized PP1 activity drives activation of Rho and Myosin II accumulation in turn.[3] Our results argue that Cul-5 and Src act in a pathway downstream or parallel to the cell cycle to regulate Rho activity. The molecular mechanisms by which Cul-5 and Src control Rho remain to be elucidated, as is the possible connection between the cell cycle oscillator and Cul-5/Src activities. Since Src has been shown to regulate Rho GTPases in several contexts via the control of guanine nucleotide exchange factors and/or GTPase-activating

203   proteins,[32-34] these proteins are natural candidates for the regulation of cortical actomyosin

204   regulation via the Cul-5/Src pathway.

205   Control of the MBT by the N/C ratio is important in several species, including *Drosophila*

206   and *Xenopus*[25,26,35-38] but likely excluding zebrafish.[39-42] This density of DNA (as well as nuclear

207   size[43,44]) can directly or indirectly impact multiple aspects of the MBT, namely zygotic gene

208   expression[45-48] and cell cycle control.[26,35,49-51] Here, we have exploited the changes in nuclear

209   positioning in *shkl* embryos to generate a continuous range of nuclear densities. This property

210   allowed us to gain insights into how the decision of nuclei to pause their cell cycles at the MBT is

211   affected by the N/C ratio. We found that the threshold for nuclear division is about 70% of the

212   density at nuclear cycle 14, which confirms previous results. This value—halfway between the

213   density at cycle 13 and 14—likely contributes to the robustness of the MBT. However, this value

214   is not sufficient for the robustness of the MBT. To ensure reliable lengthening of cycle 14 in all

215   nuclei, the sensing of the N/C ratio must be averaged over hundreds of nuclei. Consistently, our

216   results indicate that nuclei might sense the local N/C ratio in neighborhoods of ~100μm. This

217   length essentially coincides with the correlation length of the Cdk1 activity field, which is

218   established via reaction-diffusion mechanisms.[24] Additionally, we found that a model based on

219   uniform sensing of the N/C ratio fails to predict the behavior of a large fraction of nuclei (only

220   70% of nuclei are predicted correctly). However, a model assuming a slightly higher N/C ratio

221   threshold in the posterior is highly predictable (>90% prediction ability) and mainly misses the

222   behavior of nuclei at the interface between the region of extra division and that of normal division.

223   Thus, we propose that the N/C ratio is the major regulator of the cell cycle at the MBT and that no

224   mechanism other than a slight spatial modulation of the N/C threshold is needed to account for

225   nuclear behaviors. This spatial modulation likely reflects the fact that the rate of Cdk1 activation

19

226 is also slightly graded across the AP axis. The Cdk1 activation gradient is dependent on the DNA

227 replication checkpoint, which argues that the gradient might be controlled by an asymmetric

228 distribution of factors controlling DNA replication and/or Chk1 activity.[52-54] Alternatively, the

229 DNA replication checkpoint and Cdk1 activity might be influenced by factors controlling AP

230 patterning and expressed in gradients across the embryos.[55] In the future, it will be interesting to

231 understand the mechanisms and possible functional significance of this gradient.

232 The precise coordination of biochemical and mechanical signals is a ubiquitous feature of

233 embryonic development. In early *Drosophila* embryogenesis, it is necessary for the uniform

234 positioning of nuclei and timing of the MBT. Our work has identified a new pathway wherein Cul-

235 5 regulates cortical contractility by restricting Src activity. Our results investigating embryos with

236 patchy divisions indicate that nuclei sense the N/C ratio in neighborhoods of ~100μm and pause

237 the cell cycle when the local density exceeds a threshold around 70% of the normal density at the

238 MBT. Moreover, the threshold required to arrest the cell cycle is slightly graded across the AP

239 axis and is coupled to the spatiotemporal dynamics of Cdk1. Quantitatively measuring biochemical

240 and physical dynamics during specific morphogenic events will undoubtedly continue to reveal

241 new insights into the mechanisms and regulations of these pathways.

242

Acknowledgments

253

254   **Author contributions**

255   Conceptualization, L.H., A.C., V.E.D., and S.D.; Methodology, L.H., A.C., V.E.D., A.P., and S.D.;

256   Software, L.H. and A.P.; Investigation, L.H., A.C., V.E.D., and A.P.; Writing – Original Draft,

257   L.H. and S.D.; Supervision, A.C and S.D. Funding Acquisition, S.D.
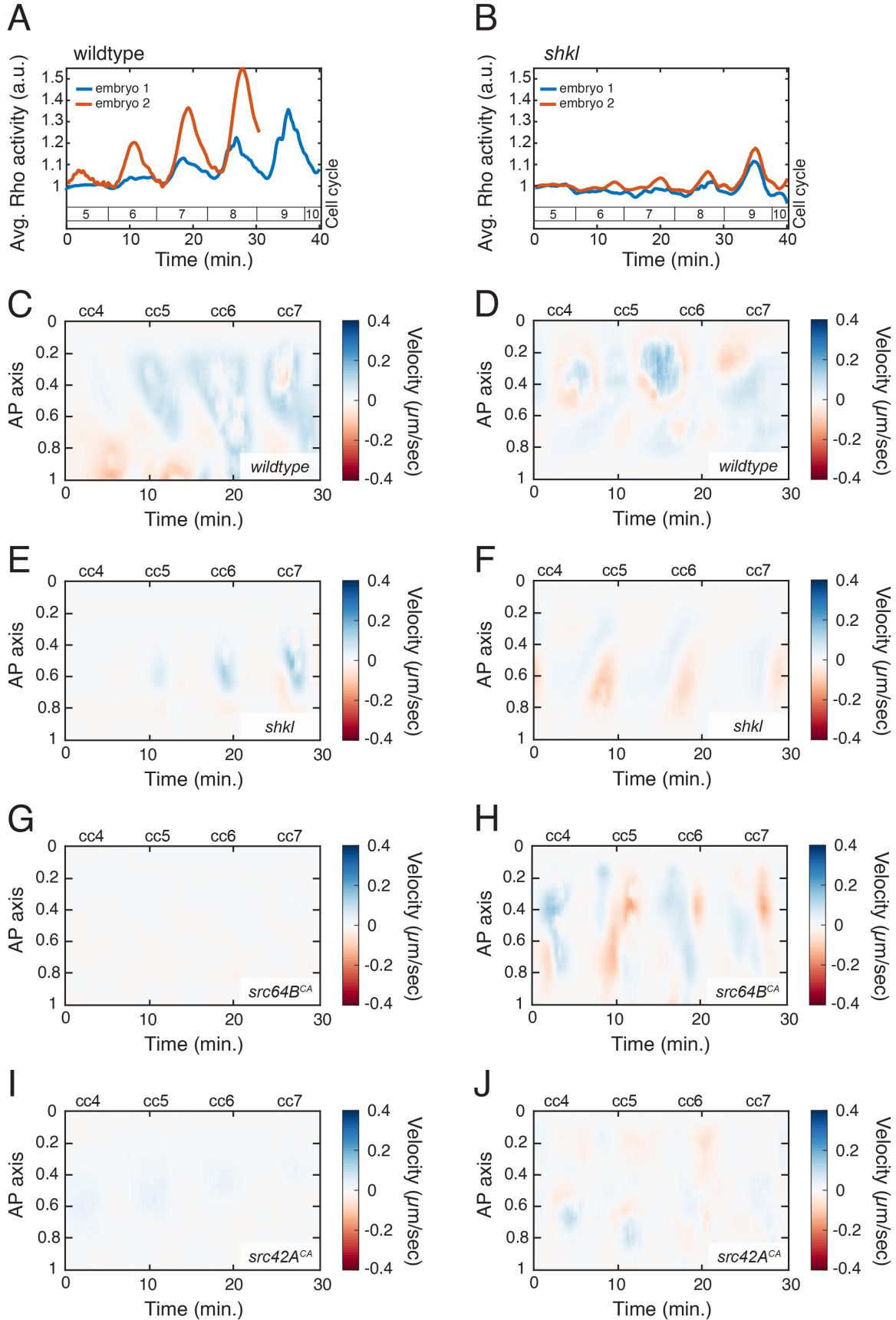
258

259   **Declaration of interests**

260   The authors declare no competing interests.
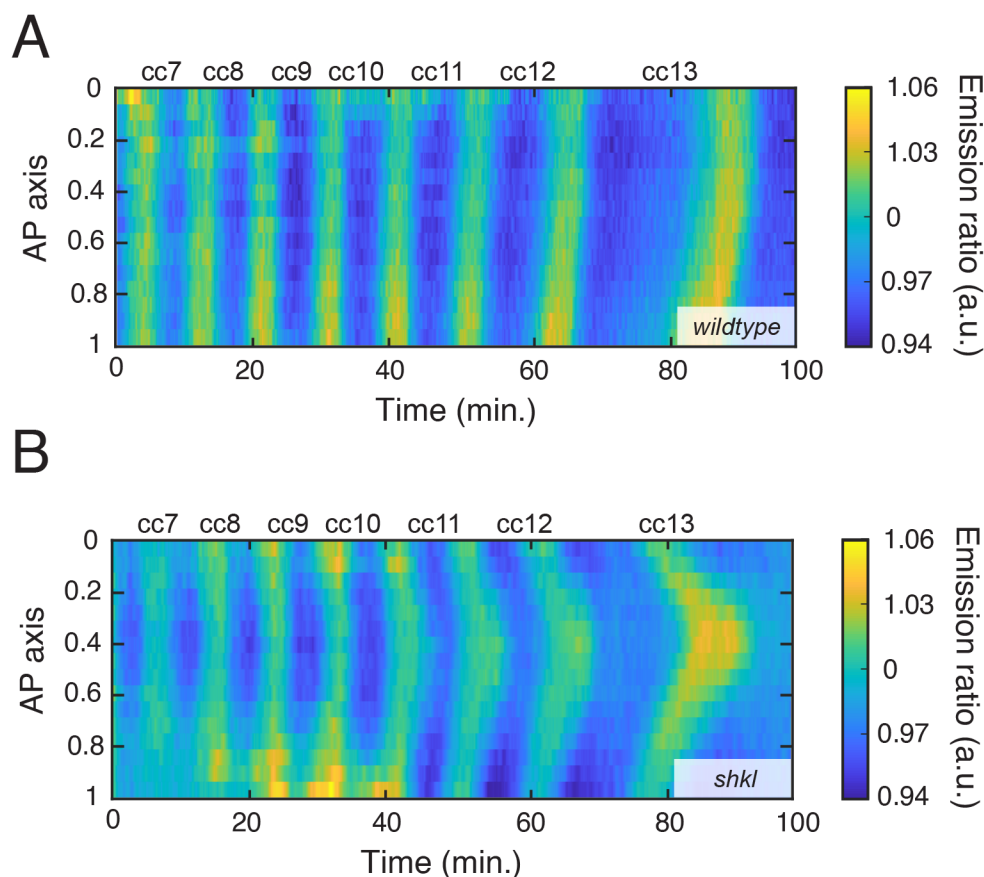
261

262   **Supplementary Figures**

263

264

21

265

266 **Fig. S1. Quantification of cortical contractility and cytoplasmic flows.** (A, B) Replicate

267 quantification of Rho activity in wildtype (A) and *shkl* (B) embryos. (C-J) Replicate heatmap

268 quantification of cytoplasmic flows in wildtype (C, D) *shkl* (E, F), src64B overexpression (G, H),

269 and src42A overexpression (I, J).

270

271

272 **Fig. S2. Spatial quantification of Cdk1/PP1 FRET sensor.** Cdk1/PP1 FRET emission ratio for

273 wildtype (A) and *shkl* (B) embryos, measured across the AP axis and time. In time, oscillations

274 are unperturbed, and cell cycle duration is unchanged. The lower nuclear density in the posterior

275 relative to the anterior lead to slightly earlier divisions and a gradual asynchrony in cell division

276 builds up over time.

23

277

278
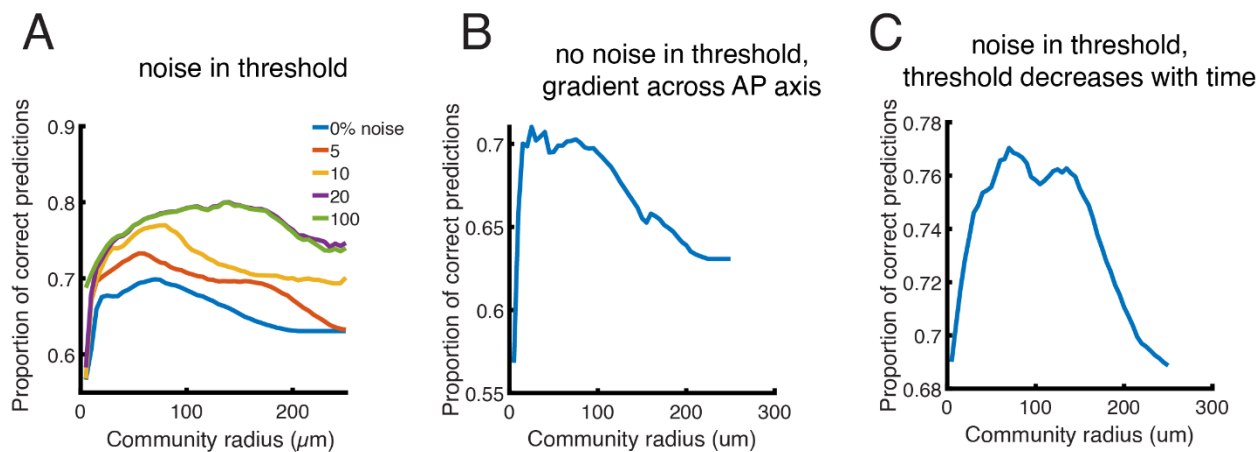
Fig. S3. Additional models of N/C ratio sensing. (A-C) Proportion of correct predictions in

possible models of N/C ratio sensing. (A) The decision to pause the cell cycle is determined by a

global threshold of ~70% (see main text Fig. 3E) which varies up to a certain percentage of this

threshold (colored lines). Allowing "noise" of 10% means the threshold for that embryo must fall

in the range [1/1.1 to 1.1]. (B) The decision to pause the cell cycle is determined by a global

threshold (Fig. 3E) with an additional gradient in threshold of up to 10% across the AP axis. (C)

The decision to pause the cell cycle is determined by a global threshold with noise (as in panel

B). Additionally, when the first nucleus divides, the threshold lowers at some rate over time

(tested uniformly from 0 to up to 15%/minute), making it more difficult for nuclei to divide.

288
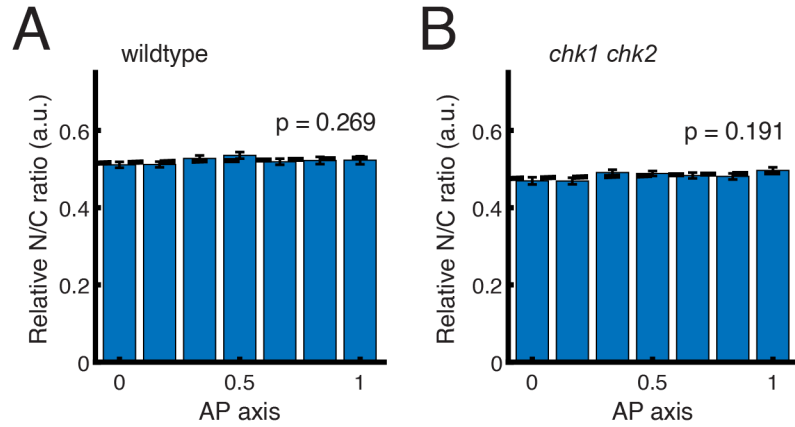
Fig. S4. Nuclear density across the AP axis. (A, B) N/C ratio (relative to the embryo's anterior) across the AP axis in wildtype (A) and *chk1 chk2* (B) embryos. P-values (F-test) for the significance of the slope are shown and indicate a uniform nuclear density across the AP axis for both genotypes.

References

1. Gerhart, J.C. (1980). Mechanisms Regulating Pattern Formation in the Amphibian Egg and Early Embryo. In Biological Regulation and Development, R. Goldberger, ed. (Plenum Press), pp. 133-316.
2. Zalokar, M., and Erk, I. (1976). Division and migration of nuclei during early embryogenesis of Drosophila melanogaster. J.Microsc.Biol.Cell. *25*, 97-106.
3. Deneke, V.E., Puliafito, A., Krueger, D., Narla, A.V., De Simone, A., Primo, L., Vergassola, M., De Renzis, S., and Di Talia, S. (2019). Self-Organized Nuclear Positioning Synchronizes the Cell Cycle in *Drosophila* Embryos. Cell *177*, 925-941.e917. 10.1016/j.cell.2019.03.007.
4. Yohn, C.B., Pusateri, L., Barbosa, V., and Lehmann, R. (2003). l (3) malignant brain tumor and three novel genes are required for Drosophila germ-cell formation. Genetics *165*, 1889-1900.
5. Hatanaka, K., and Okada, M. (1991). Retarded nuclear migration in Drosophila embryos with aberrant F-actin reorganization caused by maternal mutations and by cytochalasin treatment. Development *111*, 909-920. 10.1242/dev.111.4.909.
6. Sarikas, A., Hartmann, T., and Pan, Z.-Q. (2011). The cullin protein family. Genome Biology *12*, 220. 10.1186/gb-2011-12-4-220.
7. Alphey, L., Jimenez, J., White-Cooper, H., Dawson, I., Nurse, P., and Glover, D.M. (1992). twine, a cdc25 homolog that functions in the male and female germline of drosophila. Cell *69*, 977-988. 10.1016/0092-8674(92)90616-K.

314   8.   Royou, A., Sullivan, W., and Karess, R. (2002). Cortical recruitment of nonmuscle myosin II in
315   early syncytial Drosophila embryos: its role in nuclear axial expansion and its regulation by Cdc2
316   activity. The Journal of cell biology *158*, 127-137.
317   9.   Munjal, A., Philippe, J.-M., Munro, E., and Lecuit, T. (2015). A self-organized biomechanical
318   network drives shape changes during tissue morphogenesis. Nature *524*, 351-355.
319   10.   Deneke, Victoria E., Melbinger, A., Vergassola, M., and Di Talia, S. (2016). Waves of Cdk1 Activity
320   in S Phase Synchronize the Cell Cycle in Drosophila Embryos. Developmental Cell *38*, 399-412.
321   https://doi.org/10.1016/j.devcel.2016.07.023.
322   11.   Gavet, O., and Pines, J. (2010). Progressive Activation of CyclinB1-Cdk1 Coordinates Entry to
323   Mitosis. Developmental Cell *18*, 533-543. https://doi.org/10.1016/j.devcel.2010.02.013.
324   12.   Okumura, F., Joo-Okumura, A., Nakatsukasa, K., and Kamura, T. (2016). The role of cullin 5-
325   containing ubiquitin ligases. Cell Division *11*, 1. 10.1186/s13008-016-0016-3.
326   13.   Laszlo, G.S., and Cooper, J.A. (2009). Restriction of Src Activity by Cullin-5. Current Biology *19*,
327   157-162. 10.1016/j.cub.2008.12.007.
328   14.   Pan, Q., Qiao, F., Gao, C., Norman, B., Optican, L., and Zelenka, P.S. (2011). Cdk5 targets active
329   Src for ubiquitin-dependent degradation by phosphorylating Src(S75). Cellular and Molecular
330   Life Sciences *68*, 3425. 10.1007/s00018-011-0638-1.
331   15.   Teckchandani, A., Laszlo, G.S., Simó, S., Shah, K., Pilling, C., Strait, A.A., and Cooper, J.A. (2014).
332   Cullin 5 destabilizes Cas to inhibit Src-dependent cell transformation. Journal of Cell Science *127*,
333   509-520. 10.1242/jcs.127829.
334   16.   Hakak, Y., and Martin, G.S. (1999). Ubiquitin-dependent degradation of active Src. Current
335   Biology *9*, S1-1042. 10.1016/S0960-9822(99)80453-9.
336   17.   Harris, K.F., Shoji, I., Cooper, E.M., Kumar, S., Oda, H., and Howley, P.M. (1999). Ubiquitin-
337   mediated degradation of active Src tyrosine kinase. Proceedings of the National Academy of
338   Sciences *96*, 13738-13743.
339   18.   Imamoto, A., and Soriano, P. (1993). Disruption of the csk gene, encoding a negative regulator of
340   Src family tyrosine kinases, leads to neural tube defects and embryonic lethality in mice. Cell *73*,
341   1117-1124. 10.1016/0092-8674(93)90641-3.
342   19.   Brown, M.T., and Cooper, J.A. (1996). Regulation, substrates and functions of src. Biochimica et
343   biophysica acta *1287 2-3*, 121-149.
344   20.   O'Reilly, A.M., Ballew, A.C., Miyazawa, B., Stocker, H., Hafen, E., and Simon, M.A. (2006). Csk
345   differentially regulates Src64 during distinct morphological events in Drosophila germ cells.
346   Development *133*, 2627-2638. 10.1242/dev.02423.
347   21.   Boschek, C.B., Jockusch, B.M., Friis, R.R., Back, R., Grundmann, E., and Bauer, H. (1981). Early
348   changes in the distribution and organization of microfilament proteins during cell
349   transformation. Cell *24*, 175-184. 10.1016/0092-8674(81)90513-4.
350   22.   Pedraza, L.G., Stewart, R.A., Li, D.-M., and Xu, T. (2004). Drosophila Src-family kinases function
351   with Csk to regulate cell proliferation and apoptosis. Oncogene *23*, 4754-4762.
352   10.1038/sj.onc.1207635.
353   23.   Idema, T., Dubuis, J.O., Kang, L., Manning, M.L., Nelson, P.C., Lubensky, T.C., and Liu, A.J. (2013).
354   The Syncytial Drosophila Embryo as a Mechanically Excitable Medium. PLOS ONE *8*, e77216.
355   10.1371/journal.pone.0077216.
356   24.   Vergassola, M., Deneke, V.E., and Di Talia, S. (2018). Mitotic waves in the early embryogenesis of
357   Drosophila: Bistability traded for speed. Proceedings of the National Academy of Sciences *115*,
358   E2165-E2174. 10.1073/pnas.1714873115.
359   25.   Lu, X., Li, J.M., Elemento, O., Tavazoie, S., and Wieschaus, E.F. (2009). Coupling of zygotic
360   transcription to mitotic control at the Drosophila mid-blastula transition. Development *136*,
361   2101-2110. 10.1242/dev.034421.

362   26.   Edgar, B.A., Kiehle, C.P., and Schubiger, G. (1986). Cell cycle control by the nucleo-cytoplasmic
363   ratio in early Drosophila development. Cell *44*, 365-372. https://doi.org/10.1016/0092-
364   8674(86)90771-3.
365   27.   Chang, J.B., and Ferrell Jr, J.E. (2013). Mitotic trigger waves and the spatial coordination of the
366   Xenopus cell cycle. Nature *500*, 603-607.
367   28.   Novak, B., and Tyson, J.J. (1993). Modeling the cell division cycle: M-phase trigger, oscillations,
368   and size control. Journal of theoretical biology *165*, 101-134.
369   29.   Fogarty, P., Campbell, S.D., Abu-Shumays, R., Phalle, B.d.S., Yu, K.R., Uy, G.L., Goldberg, M.L.,
370   and Sullivan, W. (1997). The Drosophila grapes gene is related to checkpoint gene chk1/rad27
371   and is required for late syncytial division fidelity. Current Biology *7*, 418-426.
372   https://doi.org/10.1016/S0960-9822(06)00189-8.
373   30.   Sibon, O.C.M., Stevenson, V.A., and Theurkauf, W.E. (1997). DNA-replication checkpoint control
374   at the Drosophila midblastula transition. Nature *388*, 93-97. 10.1038/40439.
375   31.   Shimuta, K., Nakajo, N., Uto, K., Hayano, Y., Okazaki, K., and Sagata, N. (2002). Chk1 is activated
376   transiently and targets Cdc25A for degradation at the Xenopus midblastula transition. The
377   EMBO journal *21*, 3694-3703.
378   32.   Brouns, M.R., Matheson, S.F., and Settleman, J. (2001). p190 RhoGAP is the principal Src
379   substrate in brain and regulates axon outgrowth, guidance and fasciculation. Nature Cell Biology
380   *3*, 361-367. 10.1038/35070042.
381   33.   DerMardirossian, C., Rocklin, G., Seo, J.-Y., and Bokoch, G.M. (2006). Phosphorylation of RhoGDI
382   by Src regulates Rho GTPase binding and cytosol-membrane cycling. Mol Biol Cell *17*, 4760-4768.
383   10.1091/mbc.e06-06-0533.
384   34.   Nagao, M., Kaziro, Y., and Itoh, H. (1999). The Src family tyrosine kinase is involved in Rho-
385   dependent activation of c-Jun N-terminal kinase by Gα12. Oncogene *18*, 4425-4434.
386   10.1038/sj.onc.1202832.
387   35.   Newport, J., and Kirschner, M. (1982). A major developmental transition in early xenopus
388   embryos: I. characterization and timing of cellular changes at the midblastula stage. Cell *30*, 675-
389   686. 10.1016/0092-8674(82)90272-0.
390   36.   Newport, J., and Kirschner, M. (1982). A major developmental transition in early xenopus
391   embryos: II. control of the onset of transcription. Cell *30*, 687-696. 10.1016/0092-
392   8674(82)90273-2.
393   37.   Masui, Y., and Wang, P. (1998). Cell cycle transition in early embryonic development of Xenopus
394   laevis. Biology of the Cell *90*, 537-548. https://doi.org/10.1111/j.1768-322X.1998.tb01062.x.
395   38.   Edgar, B.A., and Schubiger, G. (1986). Parameters controlling transcriptional activation during
396   early drosophila development. Cell *44*, 871-877. 10.1016/0092-8674(86)90009-7.
397   39.   Chan, S.H., Tang, Y., Miao, L., Darwich-Codore, H., Vejnar, C.E., Beaudoin, J.-D., Musaev, D.,
398   Fernandez, J.P., Benitez, M.D.J., Bazzini, A.A., et al. (2019). Brd4 and P300 Confer Transcriptional
399   Competency during Zygotic Genome Activation. Developmental Cell *49*, 867-881.e868.
400   10.1016/j.devcel.2019.05.037.
401   40.   Lee, M.T., Bonneau, A.R., Takacs, C.M., Bazzini, A.A., DiVito, K.R., Fleming, E.S., and Giraldez, A.J.
402   (2013). Nanog, Pou5f1 and SoxB1 activate zygotic gene expression during the maternal-to-
403   zygotic transition. Nature *503*, 360-364. 10.1038/nature12632.
404   41.   Pálfy, M., Joseph, S.R., and Vastenhouw, N.L. (2017). The timing of zygotic genome activation.
405   Current Opinion in Genetics & Development *43*, 53-60.
406   https://doi.org/10.1016/j.gde.2016.12.001.
407   42.   Gert, K.R., Quio, L.E.C., Novatchkova, M., Guo, Y., Cairns, B.R., and Pauli, A. (2021). Reciprocal
408   zebrafish-medaka hybrids reveal maternal control of zygotic genome activation timing. bioRxiv,
409   2021.2011.2003.467109. 10.1101/2021.11.03.467109.

410   43.   Jevtić, P., and Levy, D.L. (2017). Both Nuclear Size and DNA Amount Contribute to Midblastula
411   Transition Timing in Xenopus laevis. Scientific Reports *7*, 7908. 10.1038/s41598-017-08243-z.
412   44.   Jevtić, P., and Levy, D.L. (2015). Nuclear size scaling during Xenopus early development
413   contributes to midblastula transition timing. Curr Biol *25*, 45-52. 10.1016/j.cub.2014.10.051.
414   45.   Syed, S., Wilky, H., Raimundo, J., Lim, B., and Amodeo, A.A. (2021). The nuclear to cytoplasmic
415   ratio directly regulates zygotic transcription in Drosophila through multiple modalities. Proc Natl
416   Acad Sci U S A *118*, e2010210118. 10.1073/pnas.2010210118.
417   46.   Lee, M.T., Bonneau, A.R., and Giraldez, A.J. (2014). Zygotic Genome Activation During the
418   Maternal-to-Zygotic Transition. Annual Review of Cell and Developmental Biology *30*, 581-613.
419   10.1146/annurev-cellbio-100913-013027.
420   47.   Pritchard, D.K., and Schubiger, G. (1996). Activation of transcription in Drosophila embryos is a
421   gradual process mediated by the nucleocytoplasmic ratio. Genes & Development *10*, 1131-1142.
422   10.1101/gad.10.9.1131.
423   48.   Jukam, D., Kapoor, R.R., Straight, A.F., and Skotheim, J.M. (2021). The DNA-to-cytoplasm ratio
424   broadly activates zygotic gene expression in Xenopus. Current Biology *31*, 4269-4281.e4268.
425   10.1016/j.cub.2021.07.035.
426   49.   Farrell, J.A., and O'Farrell, P.H. (2014). From Egg to Gastrula: How the Cell Cycle Is Remodeled
427   During the Drosophila Mid-Blastula Transition. Annual Review of Genetics *48*, 269-294.
428   10.1146/annurev-genet-111212-133531.
429   50.   Blythe, Shelby A., and Wieschaus, Eric F. (2015). Zygotic Genome Activation Triggers the DNA
430   Replication Checkpoint at the Midblastula Transition. Cell *160*, 1169-1181.
431   https://doi.org/10.1016/j.cell.2015.01.050.
432   51.   Strong, I.J.T., Lei, X., Chen, F., Yuan, K., and O'Farrell, P.H. (2020). Interphase-arrested Drosophila
433   embryos activate zygotic gene expression and initiate mid-blastula transition events at a low
434   nuclear-cytoplasmic ratio. PLOS Biology *18*, e3000891. 10.1371/journal.pbio.3000891.
435   52.   Liu, B., Winkler, F., Herde, M., Witte, C.-P., and Großhans, J. (2019). A link between
436   deoxyribonucleotide metabolites and embryonic cell-cycle control. Current Biology *29*, 1187-
437   1192. e1183.
438   53.   Djabrayan, N.J.V., Smits, C.M., Krajnc, M., Stern, T., Yamada, S., Lemon, W.C., Keller, P.J.,
439   Rushlow, C.A., and Shvartsman, S.Y. (2019). Metabolic Regulation of Developmental Cell Cycles
440   and Zygotic Transcription. Current Biology *29*, 1193-1198.e1195.
441   https://doi.org/10.1016/j.cub.2019.02.028.
442   54.   Shindo, Y., and Amodeo, A.A. (2021). Excess histone H3 is a competitive Chk1 inhibitor that
443   controls cell-cycle remodeling in the early Drosophila embryo. Current Biology *31*, 2633-
444   2642.e2636. 10.1016/j.cub.2021.03.035.
445   55.   Gilbert, S.F. (2000). Developmental biology (Sinauer Associates).

446